The Generation of Lump Solitons by a Bottom Topography in a Surface-tension Dominated Flow

Zhiming Lu and Yulu Liu

Shanghai Institute of Applied Mathematics and Mechanics, Shanghai University, Shanghai 200072, China

Reprint requests to Dr. Z. L.; E-mail: zmlu@staff.shu.edu.cn

Z. Naturforsch. **60a,** 328 – 334 (2005); received January 26, 2005

The generation of lump solitons by a three-dimensional bottom topography is numerically investigated by use of a forced Kadomtsev-Petviashvili-I (KP-I) equation. The numerical method is based on the third order Runge-Kutta method and the Crank-Nicolson scheme. The main result is the pairwise periodic generation of two pairs of lump-type solitons downstream of the obstacle. The pair with the smaller amplitude is generated with a longer period and moves in a larger angle with respect to the positive x-axis than the one with the larger amplitude. Furthermore, the effects of the detuning parameter on the generation and evolution of lumps are studied. Finally the waves propagating upstream of the obstacle are also briefly investigated.

Key words: Kadomtsev-Petviashvili-I Equation; Lump Soliton; Bottom Topography.

1. Introduction

The homogeneous Kadomtsev-Petviashvili (KP) equation

$$\frac{\partial}{\partial x}\left(\frac{\partial u}{\partial t}+6u\cdot\frac{\partial u}{\partial x}+\frac{\partial^3 u}{\partial x^3}\right)+3\sigma^2\frac{\partial^2 u}{\partial y^2}=0, \quad (1)$$

is one of the prototype equations with wide applications in modern physics of nonlinear waves [1]. In case of $\sigma^2=-1$, (1) is usually called KP-I equation. The KP-I equation arises in the case of negative dispersion, e. g., in a surface-tension dominated free surface flow. The derivation of the KP-I equation can be found in many papers [see the monograph by Albowitz and Clarkson (1991) for the derivation of the KP-I equation in a water wave problem]. The KP-I equation admits a family of lump solitons, which are localized in all directions, and which decay as x^{-2}, y^{-2}. The lump solitons have been widely investigated since they were first found numerically [2] and separately by a direct method [3]. A striking property of the interaction of two lump solitons is that not only does each soliton retain its shape and initial parameters (amplitude, velocity, size) after the collision, but its phase shift also turns out to be zero (which is unique in comparison to the collision of two solitons of the Korteweg-de Vries equation). But it does not mean that the interaction of two (or more) such solitons is as trivial as the superposition of their individual fields. Pelinnovskii and Stepanyants [4], Gorshkov et al. [2] constructed a new class of lump type solitons in terms of usual lump soliton solutions and related dynamics. Surprisingly it was shown, that when the asymptotic velocity difference (of the two solitons) vanishes, the nonlinear interaction leads to an infinite phase shift of their trajectories; besides, for some number of solitons there may exist equilibrium states corresponding to bound states of individual solitons. Albowitz and Villarroel [5] also constructed this class of lump type solitons by using inverse scattering theory in combination with perturbation methods, and more properties of multilump solitons were presented and explained via scattering theory. Recently, the rich phenomena of interaction of two lumps were investigated by a finite-difference method (based on the third order Runge-Kutta method and the Crank-Nicolson scheme, [6]). However, the generation of lump solitons by the bottom topography has been rarely studied. As far as the authors know, the only work has been carried out in terms of the generalised Benney-Luke (gBL) equation taking into account the effects of surface tension and topographical forcing [7]. The purpose of this study is to investigate the generation of lumps by bottom topography in terms of the forced KP-I equation. The remainder of the paper is organised as follows: exact solutions of lump

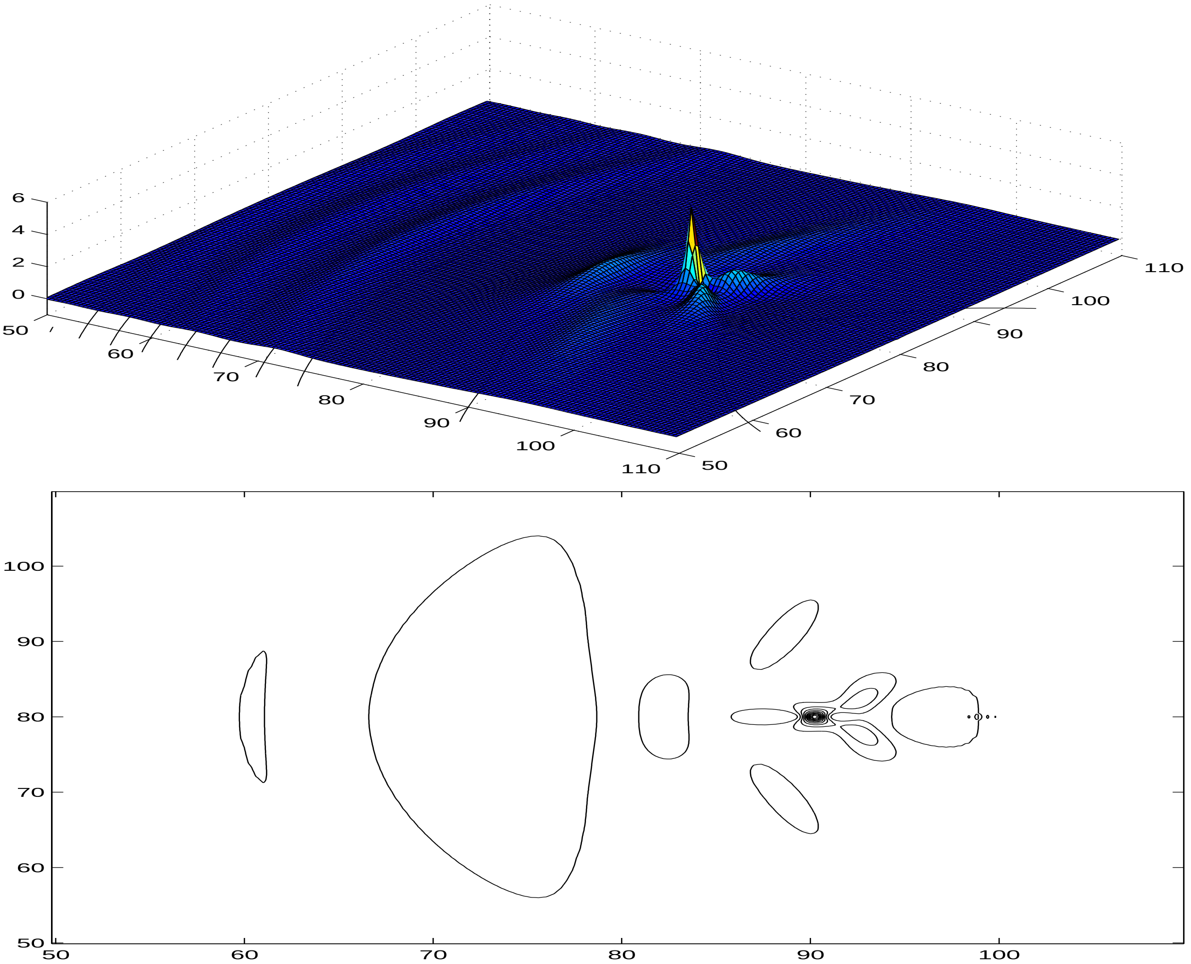

Fig. 1. Perspective view of lump solitons generated by a bottom topography at $t = 10$ (top) and the corresponding contour plot (bottom).

solitons with Horita's method are given for later comparison in Section 2, the numerical results with different detuning parameters are shown in Section 3, and finally the conclusion is given in Section 4.

2. Exact Lump Soliton Solutions

The exact solutions of the KP-I equation can be obtained by different ways. Here we write them in Hirota's form:

$$u(x,y,t) = 2\frac{\partial^2 \ln\phi}{\partial x^2}, \tag{2}$$

where ϕ is defined as

$$\phi = (\xi - 2k_{1R}\eta)^2 + 4k_{1I}^2\eta^2 + \frac{1}{4k_{1I}^2}, \tag{3}$$

and

$$u(x,y,t) = 16\frac{-4(\xi - 2k_{1R}\eta)^2 + 16k_{1I}^2\eta^2 + \frac{1}{k_{1I}^2}}{[4(\xi - 2k_{1R}\eta)^2 + 16k_{1I}^2\eta^2 + \frac{1}{k_{1I}^2}]^2}, \tag{4}$$

where

$$\xi = x - 12(k_{1R}^2 + k_{1I}^2)t, \quad \eta = y - 12k_{1R}t. \tag{5}$$

The parameters k_{1R}, k_{1I} determine the velocity and the moving direction of the lump. The initial phase of the lump soliton has been assumed to be zero without loss of generality. The amplitude of a lump soliton is defined as $\max|u|$, and the location of a lump soliton is then defined as that position where $\max|u|$ is attained. From (5), we can obtain a constraint for the slope (l)

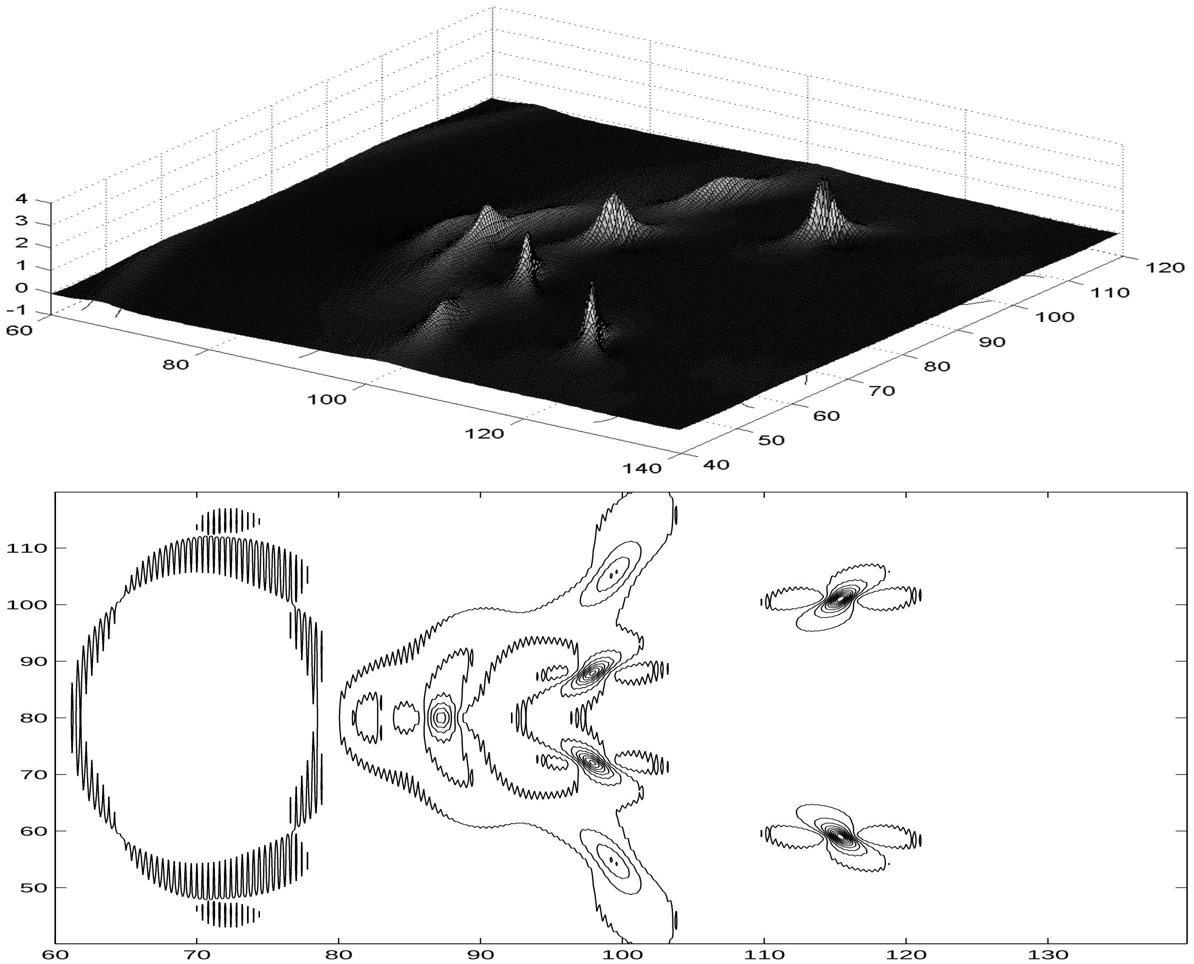

Fig. 2. Perspective view of lump solitons generated by a bottom topography at $t = 20$ (top) and the corresponding contour plot (bottom).

of the trajectory of the lump soliton as

$$l \leq \frac{1}{2k_{1I}} = \frac{2}{\sqrt{A_0}}. \tag{6}$$

That means, a lump soliton must travel within a sector of half angle (with respect to the positive x-axis) $\beta = \arctan \frac{2}{\sqrt{A_0}}$ and it is clearly seen that the angle becomes smaller with an increase of the amplitude, which will be qualitatively confirmed by the numerical results in this paper.

3. Numerical Results

The effectiveness of our numerical schemes for the KP-I equation has been demonstrated by comparison with the exact solutions of the homogeneous KP-I equation in [6]. The generation of lump solitons by a bottom topography can be described by a forced KP-I equation as below

$$\frac{\partial}{\partial x}\Big(\frac{\partial u}{\partial t} + \Delta\frac{\partial u}{\partial x} + 6u\frac{\partial u}{\partial x} + \frac{\partial^3 u}{\partial x^3}\Big) - 3\frac{\partial^2 u}{\partial y^2} = -h_{xx}(x,y), \tag{7}$$

where Δ is the detuning parameter, and $\Delta > 0$ and $\Delta < 0$ means subcritical or supercritical behavior, respectively. Note that these definitions are opposite to those used for gravity waves due to the difference in the linear dispersion relations. Without loss of generality a Gaussian-type hill is adopted here, since the different shapes of the topography only generate slight differences of the solutions near the topography, i. e.,

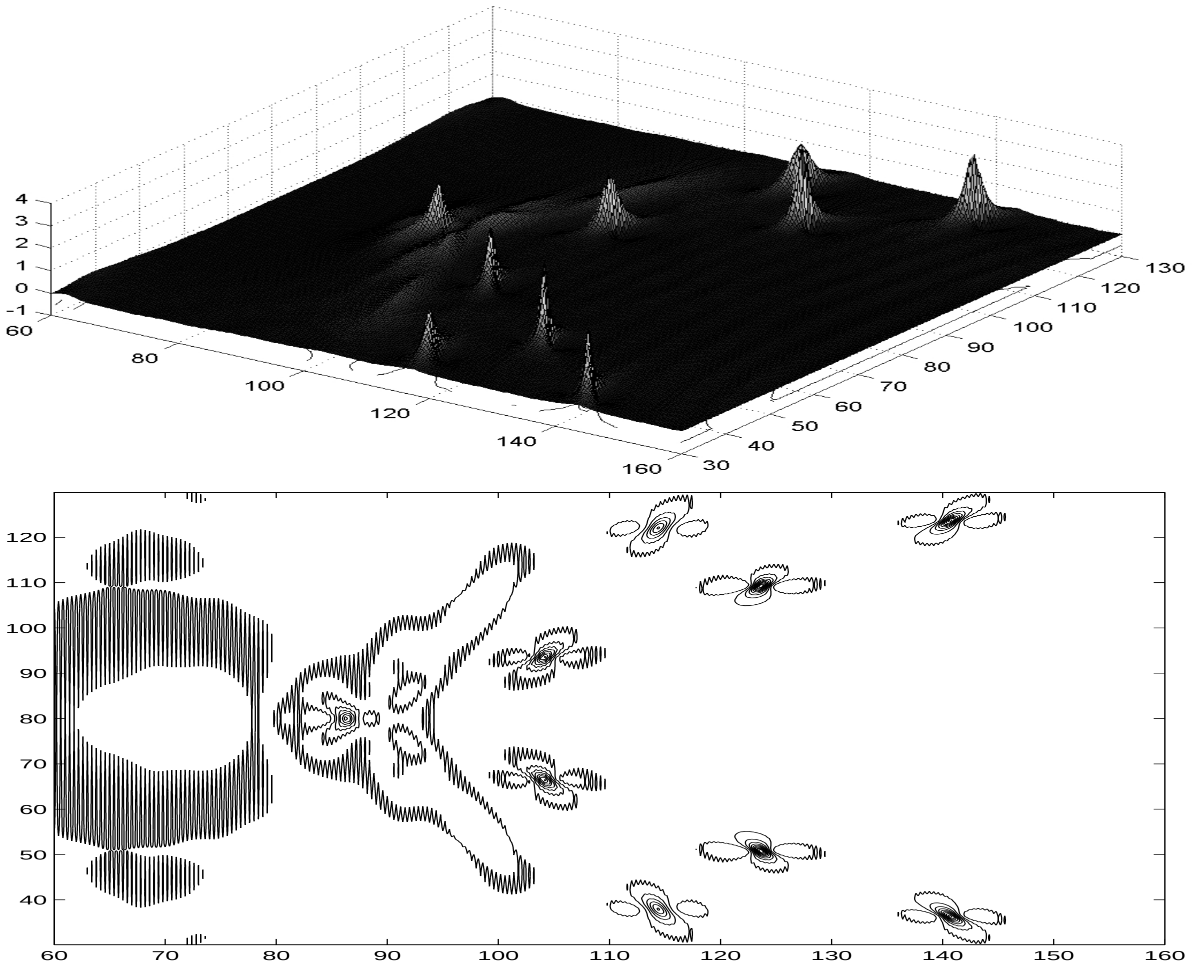

Fig. 3. Perspective view of lump solitons generated by a bottom topography at $t = 30$ (top) and the corresponding contour plot (bottom).

$H(x,y) = H_0 \exp[-\left(\frac{x-x_0}{a}\right)^2 - \left(\frac{y-y_0}{b}\right)^2]$. H_0 can be ± 1 corresponding a positive or a negative obstacle, in most simulations $a = 3$, $b = 6$, $x_0 = 80$, $y_0 = 80$ are used. The computational domain is 160 by 160, while the mesh is 800 by 801. The time step is 2.0×10^{-4}. The numerical results with $\Delta = 0$ at three different times ($t = 10$, $t = 20$, $t = 30$) are shown in Figs. 1–3, respectively. As shown in Fig. 1, a pair of lump-type solitons starts to be generated symmetrically at the positive and negative x,y-plane, while from Figs. 2 and 3 one clearly observes the symmetric pairwise periodic generation of lump-type solitons downstream of the obstacle. Note that in this case, the mean flow is from left to right, i.e., the mean flow goes to positive ∞ along the x-direction. Here, some uncertainty might arise, namely, are these humps really lump solitons described by (4)? The answer is not so straightforward since the humps vary as time goes on and we have only collected results at some discrete times. Thanks to the feature that these humps travel in a straight line in the x,y-plane, we first calculate k_{1I} from the amplitude A_0 using the formula $k_{1I} = \sqrt{A_0}/4$, then calculate k_{1R} in terms of the equation $V_{1y}/V_{1x} = l$, and finally the error between numerical results and the exact lump soliton can be calculated. It is interesting to note here again that the lump soliton must travel within a sector of half angle $\beta = \tan^{-1} 1/(2k_{1I}) = \tan^{-1} 2/\sqrt{A_0}$ with respect to the positive x-axis. Following this procedure, they are identified to be lump solitons within numerical accuracy though an interaction with the other lump solitons exists which makes the judgement a bit difficult. It is very interesting to note that we observe the peri-

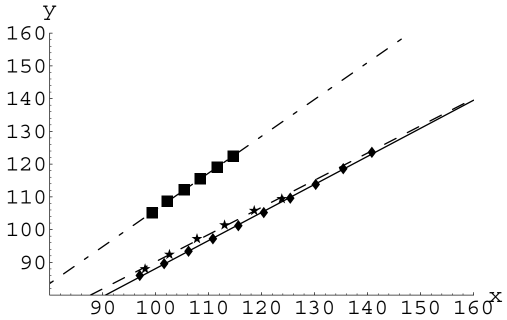

Fig. 4. The trajectories of lump solitons generated by a bottom topography (note only one of the pairs is shown): The diamonds represent the trajectory of the first lump soliton with larger amplitude from $t = 12$ to 30, while the line represents the fitted straight line; the stars represent the trajectory of the second lump soliton with larger amplitude from $t = 20$ to 30, while the dashed line is the fitted line; the squares represent the trajectory of the first lump soliton with smaller amplitude from $t = 22$ to 30, while the dash-dotted line is the fit.

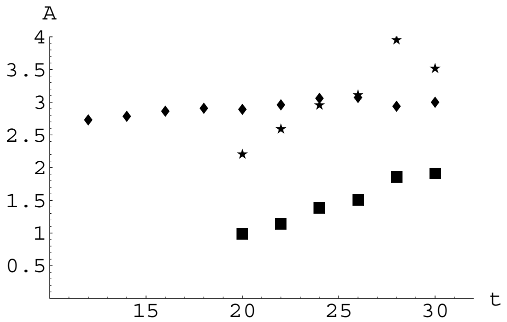

Fig. 5. The variation of the soliton amplitude with the time: The diamonds and stars represent the amplitudes of the first and the second lump soliton with larger amplitude, respectively, and the squares represent the first lump soliton with smaller amplitude.

odic generation of two pairs of lump-type solitons. The pair with the smaller amplitude seem to be generated with a longer period and moves in a larger angle to the positive x-direction than the pair with the larger amplitude. Up to the simulated time ($t = 30$), three pairs of lump solitons with larger amplitude have been generated, whereas only one pair of smaller lump solitons is clearly seen. Figure 4 shows the trajectories of the lump solitons in the x,y-plane (note only one of the pairs in the positive x,y-plane is shown), while Fig. 5 shows the time development of the amplitudes of the lump solitons. It is clearly visible that such lump solitons travel in a straight line, and in detail the trajectories of two lump solitons with larger amplitude do not coincide exactly, however, they are expected to coincide with each other as the time goes on. The angle of the trajectory with respect to the positive x-axis is about 38.85° for the pair of solitons with larger amplitude. It is interesting to note that the amplitude of the first lump changes slightly (first becomes bigger and then smaller) about the mean value of 2.92, wheareas the second one experiences a sharp variation. On the other hand, the lump soliton with smaller amplitude becomes gradually larger as the time goes on, and travels at the larger angle of 48.4°. The limiting amplitude is unknown since the computation time is too small. The pair of lump soliton of smaller amplitude is not found in the numerical solution of gBL equation and its generation mechanism appears to be different to the other pair of lump solitons, which should be further investigated.

To see the effect of the detuning parameters on the generation of the lump-type solitons, several parameters near critical regimes have been investigated (we will not show all the numerical results here). The differences of waves between two regimes are evident. This is shown in Fig. 6 with $\Delta = 0.433$ at $t = 30$ using the same bottom obstacle as before, while Fig. 7 shows the results for $\Delta = -0.433$ (note that only the solution in the positive x,y-plane is shown). Compared with Figs. 1 – 3, the main qualitative properties are the same as those of the exact resonant case, while some differences are evident, e. g. in the case of $\Delta = 0.433$ the lump solitons are of smaller amplitude, and travel in a larger angle with respect to the positive x-axis (about 44.1°). The pair of lumps with smaller amplitude is still generated but they are quite weak compared to the other pair, while in the case for $\Delta = -0.433$, the amplitude is larger (so the larger speed) than that for the exact resonant case, and the lumps travel in a smaller angle with respect to the positive x-axis (it is about 32.8°); a lump-like soliton (the detailed examination of this hump reveals that it is not a lump soliton) is also clearly seen moving along the positive x-axis, which does not exist in the case of $\Delta \leq 0$; besides, another pair of lump solitons with smaller amplitude is also seen to be generated, but with a smaller rate than that for the case of $\Delta = 0$. It is concluded that $\Delta = 0.433$ and $\Delta = -0.433$ are within the trans-critical regime.

Besides the lump solitons downstream of the obstacle, the upstream waves are also generated by the bottom obstacle. To investigate this, the upstream wave profile in the symmetrical plane ($y = 0$) for the case of $\Delta = 0$ is shown in Fig. 8 for instruction. It is clearly seen that a series of cnoidal waves with smaller am-

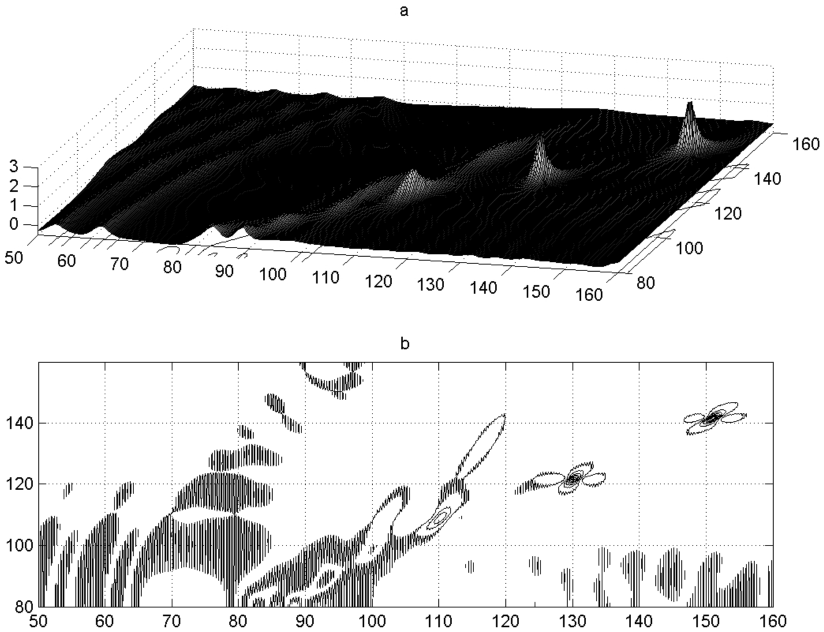

Fig. 6. A perspective view of lump solitons generated by a bottom topography with $\Delta = 0.433$ at $t = 30$ (top) and the corresponding contour plot (bottom).

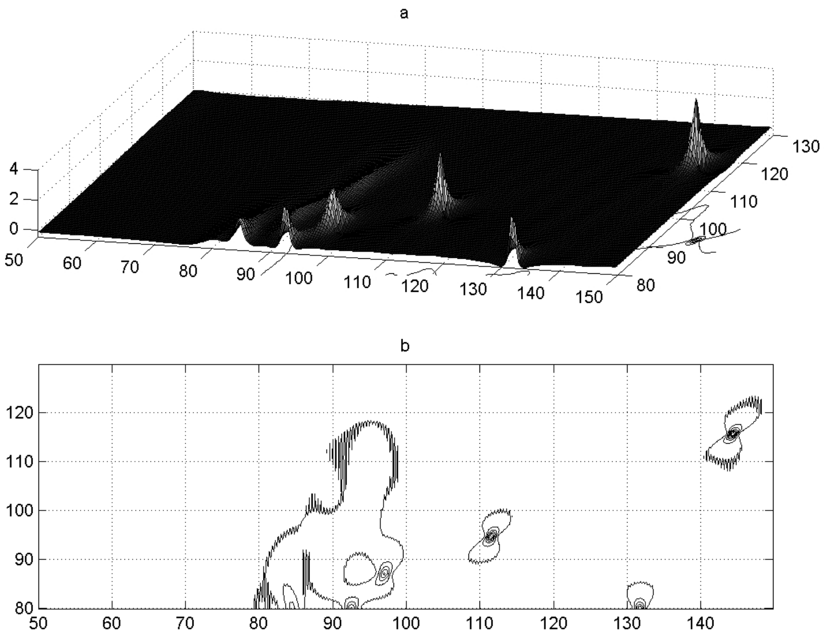

Fig. 7. A perspective view of lump solitons generated by a bottom topography with $\Delta = -0.433$ at $t = 30$ (top) and the corresponding contour plot (bottom).

plitudes leading those with larger amplitudes followed by a round depression is generated upstream of the bottom obstacle, which looks similar to the depression followed by lee waves downstream of the obstacle in an usual water wave problem (the KP-II equation applies there). It is also known from the numerical results that, unlike the downstream lump solitons, the main features of the upstream waves are the same for both $\triangle > 0$ and $\triangle < 0$, and the speed of the upstream waves become larger with the decrease of the detuning parameter.

4. Conclusions

The pair-wise periodic generation of lump solitons by bottom obstacles has been clearly demonstrated

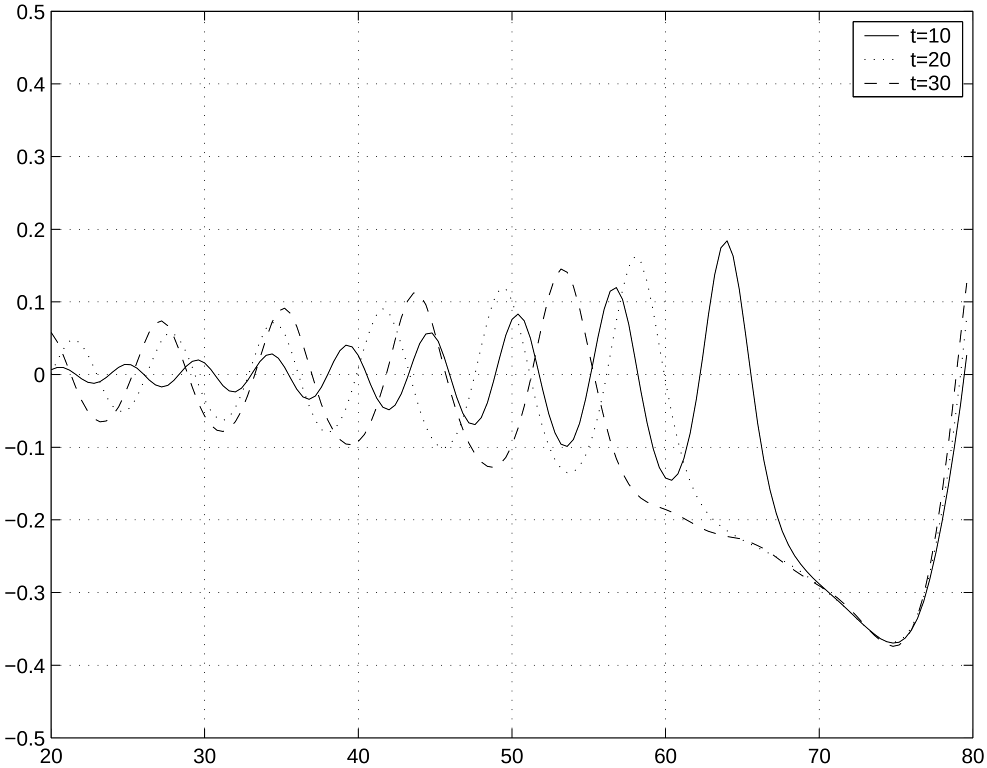

Fig. 8. The upstream-propagation waves on the symmetrical plane generated by a bottom obstacle for $\Delta = 0$.

by numerical computation of the forced KP-I equation. The pair of lump soliton of smaller amplitude was however not found in the solution of gBL equation and its generation mechanism appears to be different to the other pair of lump solitons, which should be further investigated. The lumps of smaller amplitude travel in a larger angle with respect to the positive x-axis, which, to some extent, confirms the theoretical constraint (6) for the possible trajectory of a lump soliton described by the KP-I equation. It has also been shown that the generation and later evolution of lump solitons are different for $\Delta > 0$ and $\Delta < 0$, while the properties of upstream waves are very similar for $\Delta > 0$ and $\Delta < 0$. It is expected that lump solitons will be generated asymmetrically when the bottom obstacle is inclined with respect to the mean flow direction, which has been confirmed by our preliminary numerical simulations. The detailed dependence of the generation and evolution of the lump solitons on the inclined angle of the bottom topography needs further investigation.

Acknowledgement: Z. Lu would like to thank Prof. Roger Grimshaw for his supervision to this work during his study for PhD at the Department of Mathematical Sciences, Loughborough University, UK. This work is partly supported by NSFC Grant No 10472063.

[1] M. J. Albowitz and P. A. Clarkson, Solitons, Nonlinear Evolution Equations and Inverse Scattering, Cambridge University Press, Cambridge 1991.
[2] K. A. Gorshkov, D. E. Pelinnovskii, and Y. A. Stepanyants, JETP **77**, 237 (1993).
[3] S. V. Manakov, V. E. Zakhorov, L. A. Bordag, A. R. Its, and V. B. Matveev, Phys. Lett. **63**, 205 (1977).
[4] D. E. Pelinnovskii and Y. A. Stepanyants, JETP Lett. **57**, 24 (1993).
[5] M. J. Albowitz and J. Villarroel, Phys. Rev. Lett. **78**, 570 (1997).
[6] Z. Lu, E. M. Tian, and R. Grimshaw, Wave Motion **40**, 123 (2004).
[7] K. M. Berger and P. A. Milewski, SIAM J. Appl. Math. **61**, 731 (2000).